crystals

MDPI

Article

Modeling the Effect of Magnesium Content on the Electrical Conductivity and Hardness of Technical Aluminum (1050) Alloy

Dania Bani Hani [1], Raed Al Athamneh [2], Zaid Albataineh [1,*], Mustafa Rawashdeh [2] and Issam Makableh [3]

[1] Hijjawi Faculty for Engineering Technology, Yarmouk University, Irbid 21163, Jordan; dtbanihani@yu.edu.jo
[2] Department of Industrial Engineering, Faculty of Engineering, The Hashemite University, P.O.BOX 330127, Zarqa 13133, Jordan; raedq@hu.edu.jo (R.A.A.); mustafar@hu.edu.jo (M.R.)
[3] Faculty of Engineering, Jordan University of Science and Technology, Irbid 22110, Jordan; issam.maqableh@gmail.com
* Correspondence: zaid.bataineh@yu.edu.jo

Abstract: Aluminum alloys use is so profound in many applications such as transportation, construction, energy, defense applications, automotive, aerospace, to name a few. Therefore, investigating the mechanical and electrical properties of the different types for aluminum alloys is vital. The Al–Mg alloy is widely used in the automotive industry because of its optimal properties, for example, corrosion resistance, weldability, and strength-to-weight ratio. This study aims to investigate and model the effect of changing the magnesium percentage content on the hardness and electrical conductivity of Al–Mg alloy with a detailed statistical analysis to validate the results. The microstructure at each Mg percentile content is demonstrated using a scanning electron microscope (SEM) and an optical microscope for validating the Mg content after solidification and tracking the grain size evolutions at different Mg percentiles. Vickers hardness testing is applied for hardness evaluation at each experimental condition. The electrical conductivity is tested using a PCE 20COM electric conductive non-destructive test (NDT). Prediction models are constructed to estimate the hardness and electrical conductivity as a function of Mg percentile by using a nonlinear optimizer. The results indicated that the hardness is significantly increased with increasing the Mg content by three times when comparing 0 Mg wt.% and 5 mg wt.%. In contrast, a 48% reduction in the electrical conductivity is found when Mg wt.% is increased to 5 and a notable decrease in the grain size is observed when the Mg content is increased.

Keywords: aluminum alloy; modeling; hardness; electric conductivity; magnesium

Citation: Bani Hani, D.; Al Athamneh, R.; Albataineh, Z.; Rawashdeh, M.; Makableh, I. Modeling the Effect of Magnesium Content on the Electrical Conductivity and Hardness of Technical Aluminum (1050) Alloy. *Crystals* **2022**, *12*, 457. https://doi.org/10.3390/cryst12040457

Academic Editors: Dmitry A. Bedrov and Bolv Xiao

Received: 22 February 2022
Accepted: 23 March 2022
Published: 25 March 2022

1. Introduction

One of the major metal alloys that are commonly used in different industrial applications is Al alloys, due to their properties, for instance, formability, strength-to-weight ratio, corrosion resistance, and weldability [1–4]. Different types of Al alloys are widely used in numerous industrial applications, such as aerospace, automotive, construction, marine fabrication industries, electrical engineering, and biomedical applications [5–11]. Most Al alloys have superior mechanical and electrical properties compared with Al (1050) alloy properties. Al alloys are significantly influenced by the microstructure evolutions due to the changes in the chemical formula. Some important aspects when describing the microstructure include the composition of the material in terms of alloying elements in a solid solution, volume, size, shape, and types of second-phase molecules. These constitutional characteristics are summarized conveniently as microchemistry, which influences both physical and mechanical properties of materials of non-heat-treatable Al alloys [12]. Several studies have explored the mechanical and electrical properties for various Al alloys at different real operating conditions. Zhang et al. investigated the mechanical properties

and microstructure for three types of Mg–Zn–Al alloys. The effect of solidification process on the phase constituents was demonstrated. Ultimate strength, yield strength, and creep resistance were examined at room and elevated temperatures. All experimental alloys showed high creep resistance at elevated temperatures [13]. Cao and Wessen determined the effect of microstructure parameters of Mg–Al alloy on its mechanical properties. Significant effects were observed of grain size, eutectic fraction, and eutectic morphology on the ultimate strength, fracture elongation, yield strength, and hardness [14]. The effect of stacking fault energy (SFE) on the mechanical properties and microstructure of Cu–Al alloy was demonstrated by Qu et al. A negative relationship was noticed between the SEF and strength and uniform elongation [15]. Schurack et al. studied the mechanical properties of Al–Mn–Ce/Fe and Al–Mn–Pd alloys. The deformation behavior at room temperature was determined by utilizing a constant rate compression test. The microstructure analysis was performed using X-ray diffraction and SEM. Excellent mechanical properties were achieved for both studied alloys compared with conventional Al alloy [16]. The electrical conductivity, tensile strength, and micro hardness for 7055 Al alloy were tested by Zhang et al. at different aging temperatures. A positive relationship was observed between the aging temperature and the electrical conductivity [17]. Toughness and hardness were examined for AA7075 alloy by Ozer and Karaaslan. The retrogression process was implemented at different levels of working temperature. The microstructure analysis was performed using light microscope and transmission electron microscope [18]. Valiev et al. created a new novel technology to enhance the electrical conductivity and tensile strength for Al alloys using nano-structuring technique. In this study, the grain size was refined to ultra-scale and the nanosized precipitates were formed at plastic deformation stage [19]. The effect of adding Zr to Al–Mg–Si alloy on its tensile strength, thermal resistance, and hardness were evaluated by Yuan and Liang. Different levels of the heat treatment temperature and time were applied to observe the evolutions on the mechanical properties of Al–Mg–Si alloy when adding Zr. The Arrhenius model was utilized to estimate the changes in the strength at different heat treatment conditions. A significant enhancement was found on the hardness and tensile strength at elevated heat treatment temperatures [20]. Tzeng et al. investigated the effects of Mg content on the mechanical properties and corrosion of 5000 series Al alloy using a non-destructive test. The studied Mg weight percentages were between 3–6 wt.%. The linear behavior between the mechanical properties, sound wave velocity, conductivity, and corrosion were observed. The result of their study indicates the strength, and the elongation of Al alloys were increased with the increased Mg content [21]. The effects of Mg content on the damping capacity of Mg–Al alloy were explored by Li et al. Different Mg content percentages were considered in their study (4.5, 6.5, and 9.2 wt.%). Three regions, based on strain amplitude, were considered. A constant behavior for the damping capacity was found in region 3 (high strain amplitude). On the other hand, a positive relationship was detected between the damping capacity and Mg wt.% when the middle strain amplitude was represented, whereas a negative relationship was demonstrated in the low strain amplitude region [22]. Liu et al. examined the effect of Mg content on the material strengthening of Al–Mg alloy. The 0.5 and 4.1 were the studied levels of Mg content. A high strength for A1–4.1 Mg alloy was noticed with a 800 MPa strength value [23]. In this study, the hardness and the electrical conductivity was demonstrated for Al–Mg alloy at different Mg content percentiles. Several research studies have tried to investigate the mechanical and electrical properties of Mg–Al alloys at different operating conditions, for example, Park et al., Chaubey et al., Ying et al., Pan et al., and Kim et al. [24–30]. According to the presented literature, there is a need to have a study implementing a systematic approach to investigate and model the effect of the Mg content on the microstructure, mechanical, and electrical properties of Al alloys. A detailed statistical analysis with two prediction models was provided in this study for estimating the hardness and electrical conductivity for Al alloy at different Mg content percentile levels. Advanced microstructure analysis was executed by employing the SEM and optical microscope. Gold coating was utilized in the preparation process for SEM microstructure analysis.

2. Materials and Methods

Seven main steps were implemented in processing and preparation of samples in the study. Figure 1 represents a flowchart for a summary of the followed steps. The first step includes sample preparation, which has a sequence of operations including molting, mixing, solidification, mounting, grinding, polishing, and etching. Microstructure analysis was performed using JEOL JSM-7800 F Field Emission SEM with super hybrid lens and Olympus CX22 Optical microscope. The used SEM has five axis stages with up to 200 nA probe current, upper electron detector, lower electron detector, and magnification capability up to 1,000,000×. The Olympus microscope comes with a quadruple nosepiece and 4×, 10×, 40×, and 100× oil objectives focusing plan. One-sample t-test was utilized to examine the Mg content percentile after the solidification process. Vickers hardness test and electrical conductivity were examined by using a WOL PERT 401 MVD with 0.1 µm resolution and 200 µm measuring range and a PCE 20 COM with a measuring range 0.51% to 112% IACS and 0.01 resolution in the third and fourth steps, respectively. After accumulating the data from the tests, a two-sample t-test was performed in the fifth step for each group of the data that were acquired for each sample at the same conditions. In the sixth step, a one-way ANOVA analysis was accomplished for each quality characteristic (hardness and electrical conductivity) to identify the contribution of the controllable parameter (Mg percentile) on each outcome. In the last step, two prediction models were constructed to calculate the hardness and electrical conductivity values as a function of Mg percentile. An efficient software in statistical data analysis and process improvement (Minitab 20) was used to perform all the statistical analysis in this study.

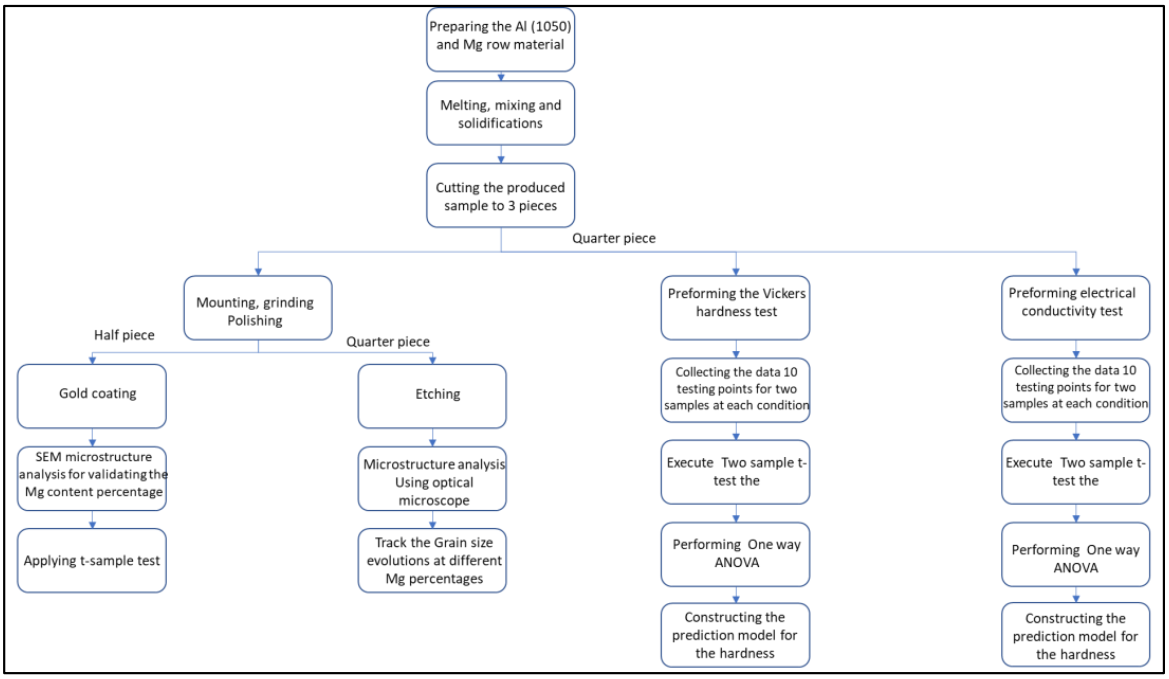

Figure 1. Case study flowchart.

Two samples of Al alloy 1050 (Al: 99.5%, Cu: 0.05%, Fe: 0.4%) with Mg were studied for different Mg content percentiles, and one sample was utilized for Al (1050) alloy. The main purpose of using two samples at each experimental condition is to validate the consistency of the mixing and solidification processes for all samples. The investigated Mg content percentiles were from 1% to 5% weight percentage (wt.%). The measurement of magnesium percentage concentration depends on weight ratio, and the percentage of each sample as a weight ratio is shown in Table 1. The casting process was performed by melting and mixing the aluminum and magnesium and then pouring the mixture into the die. After the solidification process, samples with 2.5 cm diameter and 7 mm thickness were formed

from the casting process. Each sample was cut into three pieces (one half and two quarters) where the half part was employed to measure the Mg content using SEM and the other parts were utilized for hardness and electrical conductivity tests and microstructure analysis. Different stages were implemented to prepare the samples for microstructure analysis. These stages begin from mounting the sample in the glass epoxy and then grinding for different grades and polishing. The etching process was applied only for grain size analysis using optical microscope, and the gold coating process was utilized for SEM microstructure analysis. The processes of grinding, polishing, and etching in the preparation process were used to remove the differences in the density and Mg-oxidized particles.

Table 1. Measurement of magnesium percentage concentration based on weight ratio.

Mg Concentration	Al Weight (g)	Weight Ratio	Mg Weight
1%	33.43 g 33.10 g	0.334 g 0.331 g	0.4 0.4
2%	33.32 g 33.38 g	0.666 g 0.668 g	0.8 0.8
3%	36.80 g 33.10 g	1.10 g 0.992 g	1.25 1.25
4%	33.50 g 32.13 g	1.341 g 1.280 g	1.6 1.3
5%	35.50 g 35.51 g	1.775 g 1.778 g	1.8 1.8

3. Results and Discussions

3.1. Mass Content

In order to test the mass content of the Mg inside the aluminum alloy, the scanning electron microscope (SEM) was utilized. SEM was employed for imaging minerals and other geological, biological, and environmental materials at the micrometer scale. Our JEOL JSM-7800F Field Emission SEM is equipped with secondary electron (SE) and backscattered electron (BSE) detectors. Two samples were analyzed using SEM at each Mg content percentile, at which five points were investigated for each sample. Table 2 shows the Mg content percentile in Al–Mg alloy for the two samples at each experimental condition. Figure 2 shows the measurement of mass content percentage for AL (1050) alloy with different Mg content percentiles (1%, 3%, and 5%). There was a small difference between the real and practical content. These differences are due to the Mg oxidation and the tendency of Mg to flow on the surface according to the differences in the density. Most of these parts were removed by the preparation process (grinding, polishing, and etching). The same observation was noticed at different Mg content percentiles. One-sample t-test was performed for all samples to ensure that the differences between the real and practical percentages were insignificant at a 95% confidence level. Table 3 shows one-sample t-test results for all studied samples. The p-values for all tests were more than 0.05, which indicates that there was no evidence for finding a statistically significant difference between the measured and the real values.

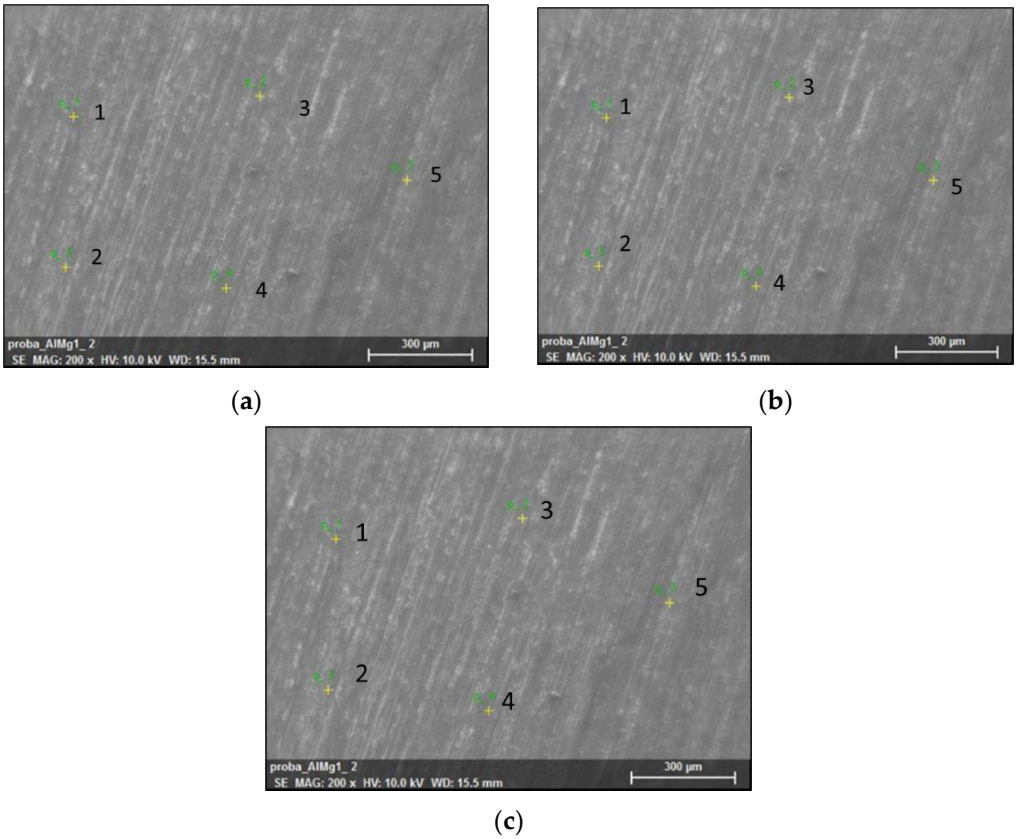

Figure 2. SEM images for Al (1050) alloy at different Mg content percentiles: (**a**) 1%; (**b**) 3%; (**c**) 5%.

Table 2. Mg content percentiles.

Testing Points	1%		2%		3%		4%		5%	
	S1	S2	S1	S2	S1	S2	S1	S2	S1	S2
1	1.04	1.08	2.04	2.11	3.09	3.13	4.04	3.9	4.97	5.13
2	0.99	0.96	2.10	1.91	3.06	2.94	4.07	4.19	5.22	5.15
3	1.09	1.07	1.98	2.07	3.11	2.98	4.14	4.01	4.94	5.08
4	0.95	1.05	2.08	2.05	3.04	3.09	4.09	3.97	5.33	4.86
5	1.03	0.97	2.09	1.97	3.10	2.95	4.17	3.92	4.89	4.93
Average	1.02	1.03	2.06	2.02	3.08	3.02	4.10	4.00	5.07	5.03
Error	0.02	0.03	0.06	0.02	0.08	0.02	0.10	0.00	0.07	0.03

Table 3. The outcomes from one-sample t-test for Mg content percentiles.

Mg Content Percentages	Null Hypothesis	Alternative Hypothesis	T-Value	*p*-Value
1%	$\mu = 1$	$\mu \neq 1$	1.4	0.194
2%	$\mu = 2$	$\mu \neq 2$	1.92	0.087
3%	$\mu = 3$	$\mu \neq 3$	2.24	0.051
4%	$\mu = 4$	$\mu \neq 4$	1.57	0.151
5%	$\mu = 5$	$\mu \neq 5$	1.01	0.337

3.2. Hardness Test Results, Analysis, and Modeling

Eleven samples were considered in this study. The first sample was Al 1050 without any Mg addition. Two samples were examined at each Mg content percentile. Ten tested points were tested for each sample. Vickers hardness test was utilized in this experiment, where 1 mm was the minimum distance between two sequential test points. A 2.5× diamond size (10 µm for 300 gf) was the considered testing setup. The hardness test unit that was used for this test is the Vickers pyramid number (HV). The main goal of testing two samples for each Mg percentage is to validate the homogeneity of all samples that were produced at each percentage. Two-sample t-test was executed at each experimental condition for confirming the homogeneity. The results of the hardness test are summarized in Table 4. A summary of the statistical test at each condition is shown in Table 5. The results of the two-sample t-test indicate that the difference between the two samples was insignificant for all Mg percentage, which means that the samples that were produced at the same condition have the same hardness performance at a 95% confidence level. The statistical evidence can be obtained from the *p*-value for each test, which is shown in Table 5, where all *p*-values were more than 0.05. As a result, failing to reject the null hypothesis of not observing a statistical difference between the two samples at each condition in all cases was observed. The pattern on the hardness behavior through Mg percentile increase was illustrated in the main effect plot in Figure 3. A notable increase in the hardness values was found when the Mg content percentile was increased. The study performed by Ibrahim et al. supports the results of this paper. A significant increase in the hardness values was found when the Mg wt.% was increased in the Al–Si–Cu–Mg alloy. This shows that the enhancement on the hardness behavior is affected by increasing the Mg wt.% content in different metal alloys [31]. One-way ANOVA analysis in Table 6 was performed to define the significance and contribution of the effect of Mg percentage on the hardness value. Based on the *p*-value (<0.001), the Mg content percentile has a significant effect on the hardness of the Al alloy. Depending on the observed pattern of the hardness, a prediction equation (Equation (1)) was constructed to estimate the hardness value as a function of Mg content percentage. Symbols H and M represent the hardness value and Mg content percentage, and $K1$–$K3$ are equation constants. The power term in the equation is used to describe the observed hardness behavior from 0 to 4 Mg weight percentage, and the linear term is utilized to work as a modifier of the power curve. In addition, the constant $K3$ is used to represent the initial value of the hardness at zero Mg weight percentage. A nonlinear optimizer was utilized to find the constant values where Gurobi was implemented as an optimization method. A final prediction equation for the hardness value with a 100% R-squared value is represented in Equation (2) where the model adequacy is characterized by the R-squared value.

$$H = K1 * M^2 + K2 * M + K3 \quad (1)$$

$$H = 0.93 * M^2 + 15.59 * M + 23.71 \quad (2)$$

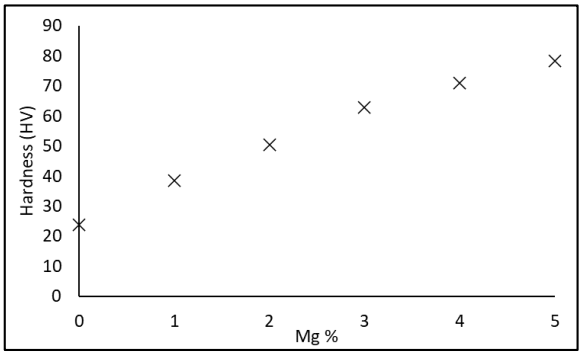

Figure 3. The hardness behavior vs. Mg content percentiles based on the averages at each condition.

Table 4. Hardness test results for Al (1050) alloy with different Mg percentiles.

Mg Concentration	Al (1050) HV	Mg 1% HV		Mg 2% HV		Mg 3% HV		Mg 4% HV		Mg 5% HV	
Num#	S	S1	S2	S1	S2	S1	S2	S1	S2	S1	S2
1	22.9	39.4	36.8	51.4	53.4	53.4	64.5	76.8	77	82.4	77.9
2	23.7	38.7	38.5	52.7	52.8	60.1	49.6	73.3	69.3	74.5	80.4
3	22.9	38.2	38.7	52.5	50.8	59.3	62.7	72.2	61.8	82.3	81.7
4	23	36.4	42.3	48.2	51.4	61	64.4	70.2	69	72.3	83
5	23.9	36.7	40.4	48.3	52.1	66.3	62.7	73.4	71.8	81.2	80.4
6	23.4	38.4	39.7	54.4	50.2	57.7	65.3	69.2	71.8	72.3	83
7	23.1	39.6	39.2	45	50.2	62.7	64.4	77.9	62.2	71.2	80.4
8	24.4	37.8	37.9	48.7	49.6	65.3	67.2	65.3	73.5	77.2	79.1
9	26.2	38.1	38.5	49.5	52.8	65.3	65.3	72.2	65.5	79.4	77.9
10	24.6	37.3	35.7	46.5	49.6	65.3	73.3	76.7	72.6	78.4	71.2
Average	23.8	38.1	38.8	49.7	51.3	61.6	63.9	72.7	69.5	77.1	79.5
Error		−0.71		−1.57		−2.3		3.27		−2.38	

Table 5. The results of two-sample t-test for the hardness data.

Mg Content Percentages	Null Hypothesis	Alternative Hypothesis	T-Value	*p*-Value
1%	$\mu1 - \mu2 = 0$	$\mu1 - \mu2 \neq 0$	−1.06	0.307
2%	$\mu1 - \mu2 = 0$	$\mu1 - \mu2 \neq 0$	−1.51	0.157
3%	$\mu1 - \mu2 = 0$	$\mu1 - \mu2 \neq 0$	−1.01	0.327
4%	$\mu1 - \mu2 = 0$	$\mu1 - \mu2 \neq 0$	1.64	0.12
5%	$\mu1 - \mu2 = 0$	$\mu1 - \mu2 \neq 0$	−1.37	0.189

Table 6. One-way ANOVA for the effect of Mg percentage on the hardness values.

		Analysis of Variance			
Source	DF	Adj SS	Adj MS	F-Value	*p*-Value
Mg %	5	32,487	6497.44	495.09	<0.001
Error	104	1365	13.12	—	—
Total	109	33,852	—	—	—

3.3. Electrical Conductivity Test Results, Analysis, and Modeling

Demonstrating the evolutions in the electrical conductivity was the main objective of this test. A PCE-COM 20 portable handheld non-destructive conductivity tester for metals was utilized to examine the electrical conductivity of Al (1050) alloy. Two samples were considered for testing at each experimental condition. Table 7 represents the values of electrical conductivity at different Mg content percentages. Five testing points were studied for each sample. Two-sample t-test was applied for each Mg percentage to verify the sampling process. Table 8 summarizes the outcomes from the two-sample t-test. No significant statistical differences were observed between the two tested samples, according to the *p*-values (>0.05) at a confidence level of 95%. Based on the results from the two-sample t-test, the samples that are operated at the same Mg percentage behaved identically regarding the electrical conductivity. The relationship between Mg content percentages and the electrical conductivity behavior is illustrated in the main effect plot in Figure 4. An obvious negative relationship was recognized between the electrical conductivity and the Mg content percentiles. The obtained results are supported by Cui et al.'s study, where the electrical conductivity of three different alloys (Al–0.5Fe–0.2Si, Al–0.5Mg–0.35Si, Al–0.8Fe–0.2Cu) was examined. The lowest value of the electrical conductivity was found for the alloy that had 0.5 wt.% Mg in its content [32]. Therefore, the negative

impact of adding Mg to the electrical conductivity for some metal alloys was identified by literature [33]. The significance and the contribution of the effects for changing the Mg percentage in Al (1050) alloy were inspected by using a one-way ANOVA. The effect of Mg content percentage on the electrical conductivity values was statistically significant according to ANOVA results, as shown in Table 9. This conclusion was realized based on the *p*-value, where the ANOVA showed a *p*-value less than 0.001 with a confidence level of 95%. A model for estimating the electrical conductivity values was built as a function of Mg percentage based on the observed pattern. Equation (3) defines the main equation elements for the suggested prediction model where E and M symbolize the electrical conductivity and Mg content percentage values, and $K1$ to $K3$ are the equation constants. The observed reduction behavior in the electrical conductivity from 0 to 3 Mg wt.% was illustrated in the power term from Equation (3). The linear term was utilized to describe the electrical conductivity behavior when Mg weight percentage is more than 3%. $K3$ represents the electrical conductivity at 0 Mg wt.%. The final equation was constructed by using a nonlinear optimizer (Gurobi). The final model was illustrated in Equation (4) with a 99% R-squared value for the prediction model. Although the prediction models for the hardness and the electrical conductivity had a high R squared value with an acceptable accuracy, there is enough margin for errors in both models. This is because of the fabrication process of Al 1050 alloy with mixing with Mg. Moreover, the solidification process has several uncontrollable factors that can cause noise for the hardness and the electrical conductivity values even when having a constant percentage of Mg content.

$$E = K1 * M^2 + K2 * M + K3 \quad (3)$$

$$E = 0.97 * M^2 - 10.19 * M + 55 \quad (4)$$

Table 7. Electrical conductivity test results for Al (1050) alloy with different Mg percentiles.

Mg Concentration	Al (1050) (IACS)	Mg 1% (IACS)		Mg 2% (IACS)		Mg 3% (IACS)		Mg 4% (IACS)		Mg 5% (IACS)	
	S	S1	S2	S1	S2	S1	S2	S1	S2	S1	S2
1	57.4	43.9	45	38.7	38.5	33.5	35.2	30.5	32.2	28.4	27.3
2	54.6	43.6	41.8	38.3	38.6	33.8	32.6	30.6	32.1	29.3	27.1
3	55.7	44.1	45.8	39.6	38.2	33.6	30.4	31.6	32.6	26.9	25.9
4	55.2	43.8	45.2	38.8	38.3	32.9	31.2	30.3	29.6	26.4	27.5
5	56.3	44.5	45.7	38.2	37.5	33.2	34.5	29.5	31.8	26.9	27.3
Average	55.8	43.9	44.7	38.7	38.2	33.4	32.8	30.5	31.7	27.6	27
Error		−0.72		0.5		0.62		−1.16		0.56	

Table 8. The results of two-sample t-test for the electrical conductivity values.

Mg Content Percentages	Null Hypothesis	Alternative Hypothesis	T-Value	*p*-Value
1%	$\mu1 - \mu2 = 0$	$\mu1 - \mu2 \neq 0$	−0.95	0.395
2%	$\mu1 - \mu2 = 0$	$\mu1 - \mu2 \neq 0$	1.59	0.156
3%	$\mu1 - \mu2 = 0$	$\mu1 - \mu2 \neq 0$	0.66	0.544
4%	$\mu1 - \mu2 = 0$	$\mu1 - \mu2 \neq 0$	−1.85	0.114
5%	$\mu1 - \mu2 = 0$	$\mu1 - \mu2 \neq 0$	0.91	0.399

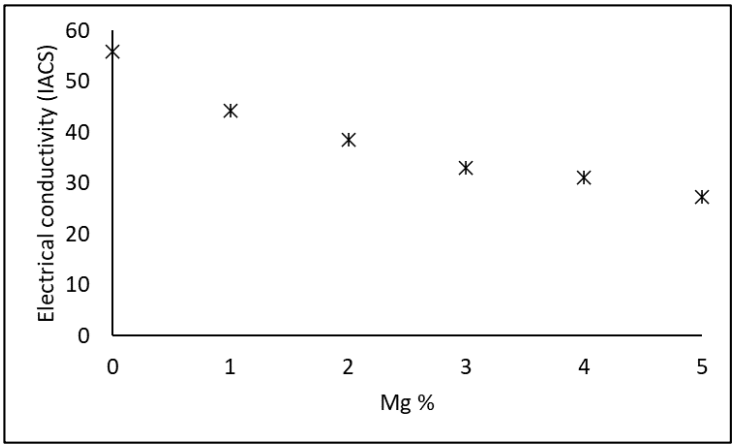

Figure 4. The electrical conductivity vs. Mg content percentiles based on the averages at each condition.

Table 9. One-way ANOVA for the effect of Mg percentage on the electrical conductivity.

Analysis of Variance					
Source	**DF**	**Adj SS**	**Adj MS**	**F-Value**	***p*-Value**
Mg %	5	3776.27	755.253	637.6	<0.001
Error	49	58.04	1.185	—	—
Total	54	3834.31	—	—	—

3.4. Microstructure Analysis

The samples were prepared for microstructure analysis using an optical microscope. Sequential processes (cutting, grinding, polishing, and etching) were implemented for these samples to prepare them for microstructure analysis. The evolutions in grain size for the Al alloy with different percentages of Mg content are examined. Figure 5 displays the changes in the grain size of Al (1050) alloy with different percentages of Mg content (0%, 1%, and 5%). The grain size was significantly decreased with increasing of the Mg content percentile in Al 1050 alloy. According to Figure 5, 60% reduction in grain size of the 1% Mg wt.% content and 80% at 5% Mg wt.% content were observed based on the three sample points that were considered to demonstrate the reduction on the grain size. In addition, the mechanical and electrical properties were directly affected by these evolutions in the grain size. The same observations were concluded by the studies of Ren et al. and Wang et al. In addition, two main precipitate types were formed when Al–Mg alloys were structured. The first precipitate form was $(FeMn)Al_6$, which is hard, insoluble, and brittle. The second type was Mg_2Al_3, which has a face-centered cubic structure with brittle behavior at room temperature [29,34]. The electrical conductivity is significantly influenced by the microstructure evolutions, where it is strongly dependent on the concentration of atoms in solid solutions. In addition, the dissolved alloying elements in metallic alloys affect the electrical resistivity in an approximately linear relationship, according to Matthiesem's rule. Moreover, the electrical conductivity is higher at the grain boundaries at which the Mg content is lower, implying a larger grain size compared to the high Mg content. The results are in accordance with the changes influenced by the microstructure evolutions [35].

Based on the experimental tests, a positive relationship was determined between the Mg content in Al 1050 alloy and the hardness value where a Vickers test was utilized to quantify the hardness of Al 1050 at different levels of Mg wt.% content. In contrast, the electrical conductivity was negatively impacted with increasing Mg content. NDT test was utilized to measure the electrical conductivity value by using a PCE-COM 20 portable hand-held non-destructive conductivity tester in IACS unit. Microstructure analysis using SEM is used to demonstrate the Mg wt.% values after the fabrication process of the experimental samples. An optical microscope was used to identify the evolutions in the microstructure

at different Mg wt.% content values. According to the experimental observations, the grain size was inversely related with Mg content percentage. Robust prediction models were built to estimate the electrical conductivity and hardness values at different Mg wt.% values. Detailed statistical analysis tools were implemented to verify the fabrication methods of the testing samples and ensure the homogeneity of the experimental conditions by using one-sample t-test and two-sample t-test. One-way ANOVA analysis was performed to ensure the contribution and significancy of the studied factors. Capability of the constructed prediction models was restricted to the range of the studied Mg wt.% contents which could be considered as a major limitation of this study. Investigating more levels of Mg wt.% to achieve a wider range of the prediction models and implementing the artificial intelligence techniques in prediction model construction can be considered in the future work.

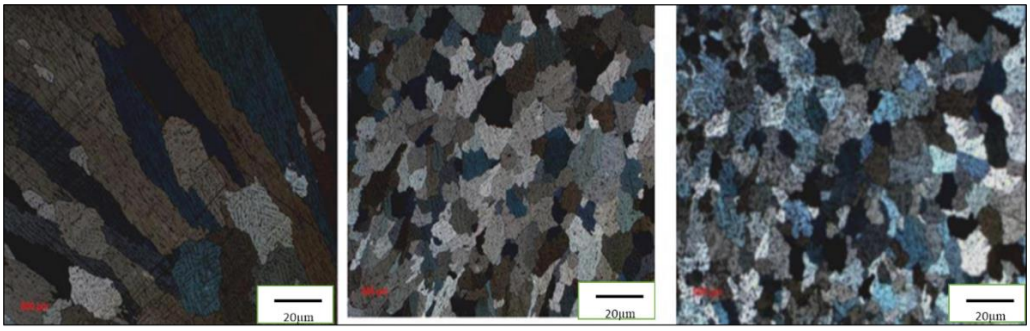

Figure 5. The evolutions in the grain sizes vs. the Mg content percentages in Al (1050) alloy: (**a**) 0%; (**b**) 1%; (**c**) 5%.

4. Conclusions

The effects of the Mg content percentiles on the hardness and electrical conductivity for Al (1050) alloy were examined in this study. Vickers hardness test and portable handheld non-destructive conductivity tester were utilized to demonstrate the evolutions in the hardness and electrical conductivity values with increasing the Mg percentage. Grain size changes were recognized using optical microscope. SEM microscope was used to confirm the accuracy of mixing and solidification processes. One-sample t-test was applied to ensure that the real Mg percentage is equal to practical Mg percentage at each experimental condition. Two-sample t-tests were examined for each Mg percentage to validate the homogeneity of the produced samples. One-way ANOVA analysis was employed to statistically illustrate the effect of Mg content percentile on the hardness and electrical conductivity performance. Ten and five testing points were considered for hardness and electrical conductivity examination. A significant increase in the hardness and an obvious reduction in the electrical conductivity and grain size were observed when the Mg percentage was increased in Al (1050) alloy. Robust prediction models were built for the hardness and the electrical conductivity values as a function of Mg content percentile with 100% and 99% R-squared values, respectively.

Author Contributions: Conceptualization, D.B.H. and R.A.A.; methodology, D.B.H.; validation, R.A.A., D.B.H. and M.R.; formal analysis, Z.A.; investigation, I.M.; resources, Z.A.; data curation, R.A.A. and D.B.H.; writing—original draft preparation, D.B.H.; writing—review and editing, Z.A. and M.R.; visualization, D.B.H.; supervision, R.A.A.; project administration, D.B.H. All authors have read and agreed to the published version of the manuscript.

Funding: This research received no external funding.

Institutional Review Board Statement: Not applicable.

Informed Consent Statement: Not applicable.

Data Availability Statement: The datasets generated during and/or analyzed during the current study are available from the corresponding author on reasonable request.

Conflicts of Interest: The authors declare no conflict of interest.

References

1. Burger, G.B.; Gupta, A.K.; Jeffrey, P.W.; Lloyd, D.J. Microstructural control of aluminum sheet used in automotive applications. *Mater. Charact.* **1995**, *35*, 23–39. [CrossRef]
2. Hirsch, J. Aluminium alloys for automotive application. *Mater. Sci. Forum* **1997**, *242*, 33–50. [CrossRef]
3. Miller, W.S.; Zhuang, L.; Bottema, J.; Wittebrood, A.; De Smet, P.; Haszler, A.; Vieregge, A.J.M.S. Recent development in aluminium alloys for the automotive industry. *Mater. Sci. Eng. A* **2000**, *280*, 37–49. [CrossRef]
4. Lloyd, D.J.; Evans, D.; Pelow, C.; Nolan, P.; Jain, M. Bending in aluminium alloys AA 6111 and AA 5754 using the cantilever bend test. *Mater. Sci. Technol.* **2002**, *18*, 621–628. [CrossRef]
5. Rambabu, P.P.N.K.V.; Prasad, N.E.; Kutumbarao, V.V.; Wanhill, R.J.H. Aluminium alloys for aerospace applications. In *Aerospace Materials and Material Technologies*; Springer: Singapore, 2017; pp. 29–52. [CrossRef]
6. Caceres, C.H. Economical and environmental factors in light alloys automotive applications. *Metall. Mater. Trans. A* **2007**, *38*, 1649–1662. [CrossRef]
7. Okulov, I.V.; Volegov, A.S.; Attar, H.; Bönisch, M.; Ehtemam-Haghighi, S.; Calin, M.; Eckert, J. Composition optimization of low modulus and high-strength TiNb-based alloys for biomedical applications. *J. Mech. Behav. Biomed. Mater.* **2017**, *65*, 866–871. [CrossRef]
8. Zhang, J.; Ma, M.; Shen, F.; Yi, D.; Wang, B. Influence of deformation and annealing on electrical conductivity, mechanical properties and texture of Al-Mg-Si alloy cables. *Mater. Sci. Eng. A* **2018**, *710*, 27–37. [CrossRef]
9. Jebaraj, A.V.; Aditya, K.V.V.; Kumar, T.S.; Ajaykumar, L.; Deepak, C.R. Mechanical and corrosion behaviour of aluminum alloy 5083 and its weldment for marine applications. *Mater. Today Proc.* **2020**, *22*, 1470–1478. [CrossRef]
10. Periasamy, K.; Sivashankar, N.; Chandrakumar, S.; Viswanathan, R. Measurement of Friction and Wear in Aluminum Alloy Al7075/Sic & Gr Processed by Friction Stir Method. *Int. J. Innov. Technol. Explor. Eng.* **2020**, *9*, 278–281. [CrossRef]
11. Merayo Fernández, D.; Rodríguez-Prieto, A.; Camacho, A.M. Prediction of the Bilinear Stress-Strain Curve of Aluminum Alloys Using Artificial Intelligence and Big Data. *Metals* **2020**, *10*, 904. [CrossRef]
12. Kabirian, F.; Khan, A.S.; Pandey, A. Negative to positive strain rate sensitivity in 5xxx series aluminum alloys: Experiment and constitutive modeling. *Int. J. Plast.* **2014**, *55*, 232–246. [CrossRef]
13. Zhang, J.; Guo, Z.X.; Pan, F.; Li, Z.; Luo, X. Effect of composition on the microstructure and mechanical properties of Mg–Zn–Al alloys. *Mater. Sci. Eng. A* **2007**, *456*, 43–51. [CrossRef]
14. Cao, H.P.; Wessén, M. Effect of microstructure on mechanical properties of as-cast Mg-Al alloys. *Metall. Mater. Trans. A* **2004**, *35*, 309–319. [CrossRef]
15. Qu, S.; An, X.H.; Yang, H.J.; Huang, C.X.; Yang, G.; Zang, Q.S.; Wang, Z.G.; Wu, S.D.; Zhang, Z.F. Microstructural evolution and mechanical properties of Cu–Al alloys subjected to equal channel angular pressing. *Acta Mater.* **2009**, *57*, 1586–1601. [CrossRef]
16. Schurack, F.; Eckert, J.; Schultz, L. Synthesis and mechanical properties of cast quasicrystal-reinforced Al-alloys. *Acta Mater.* **2001**, *49*, 1351–1361. [CrossRef]
17. Zhang, P.; Li, Y.; Liu, Y.; Zhang, Y.; Liu, J. Analysis of the microhardness, mechanical properties and electrical conductivity of 7055 aluminum alloy. *Vacuum* **2020**, *171*, 109005. [CrossRef]
18. Gokhan, O.Z.E.R.; Karaaslan, A. Properties of AA7075 aluminum alloy in aging and retrogression and reaging process. *Trans. Nonferrous Met. Soc. China* **2017**, *27*, 2357–2362. [CrossRef]
19. Valiev, R.Z.; Murashkin, M.Y.; Sabirov, I. A nanostructural design to produce high-strength Al alloys with enhanced electrical conductivity. *Scr. Mater.* **2014**, *76*, 13–16. [CrossRef]
20. Yuan, W.; Liang, Z. Effect of Zr addition on properties of Al–Mg–Si aluminum alloy used for all aluminum alloy conductor. *Mater. Des.* **2011**, *32*, 4195–4200. [CrossRef]
21. Tzeng, Y.C.; Chen, R.Y.; Lee, S.L. Nondestructive tests on the effect of Mg content on the corrosion and mechanical properties of 5000 series aluminum alloys. *Mater. Chem. Phys.* **2020**, *259*, 124202. [CrossRef]
22. Li, Z.; Yan, H.; Chen, J.; Xia, W.; Su, B.; Zhao, L.; Song, M. Effect of Mg Content on the Damping Behavior of Al–Mg Alloys. *Met. Mater. Int.* **2021**, *27*, 3155–3163. [CrossRef]
23. Liu, Y.; Liu, M.; Chen, X.; Cao, Y.; Roven, H.J.; Murashkin, M.; Valiev, R.Z.; Zhou, H. Effect of Mg on microstructure and mechanical properties of Al-Mg alloys produced by high pressure torsion. *Scr. Mater.* **2021**, *159*, 137–141. [CrossRef]
24. Park, S.H.; Kim, S.H.; Kim, Y.M.; You, B.S. Improving mechanical properties of extruded Mg–Al alloy with a bimodal grain structure through alloying addition. *J. Alloys Compd.* **2015**, *646*, 932–936. [CrossRef]
25. Chaubey, A.K.; Scudino, S.; Prashanth, K.G.; Eckert, J. Microstructure and mechanical properties of Mg–Al-based alloy modified with cerium. *Mater. Sci. Eng. A* **2015**, *625*, 46–49. [CrossRef]
26. Ying, T.; Zheng, M.Y.; Li, Z.T.; Qiao, X.G. Thermal conductivity of as-cast and as-extruded binary Mg–Al alloys. *J. Alloys Compd.* **2014**, *608*, 19–24. [CrossRef]
27. Pan, H.; Pan, F.; Wang, X.; Peng, J.; Gou, J.; She, J.; Tang, A. Correlation on the electrical and thermal conductivity for binary Mg–Al and Mg–Zn alloys. *Int. J. Thermophys.* **2013**, *34*, 1336–1346. [CrossRef]
28. Kim, S.H.; You, B.S.; Park, S.H. Effect of billet diameter on hot extrusion behavior of Mg–Al–Zn alloys and its influence on microstructure and mechanical properties. *J. Alloys Compd.* **2017**, *690*, 417–423. [CrossRef]

29. Ren, L.; Gu, H.; Wang, W.; Wang, S.; Li, C.; Wang, Z.; Zhai, Y.; Ma, P. The microstructure and properties of an Al-Mg-0.3 Sc alloy deposited by wire arc additive manufacturing. *Metals* **2020**, *10*, 320. [CrossRef]
30. Ren, L.; Gu, H.; Wang, W.; Wang, S.; Li, C.; Wang, Z.; Zhai, Y.; Ma, P. Effect of Mg content on microstructure and properties of Al–Mg alloy produced by the wire arc additive manufacturing method. *Materials* **2019**, *12*, 4160. [CrossRef]
31. Ibrahim, M.F.; Samuel, E.; Samuel, A.M.; Al-Ahmari, A.M.A.; Samuel, F.H. Metallurgical parameters controlling the microstructure and hardness of Al–Si–Cu–Mg base alloys. *Mater. Des.* **2010**, *32*, 2130–2142. [CrossRef]
32. Cui, X.; Wu, Y.; Zhang, G.; Liu, Y.; Liu, X. Study on the improvement of electrical conductivity and mechanical properties of low alloying electrical aluminum alloys. *Compos. Part B Eng.* **2011**, *110*, 381–387. [CrossRef]
33. Chen, J.K.; Hung, H.Y.; Wang, C.F.; Tang, N.K. Thermal and electrical conductivity in Al–Si/Cu/Fe/Mg binary and ternary Al alloys. *J. Mater. Sci.* **2017**, *50*, 5630–5639. [CrossRef]
34. Wang, B.; Yang, G.; Zhou, S.; Cui, C.; Qin, L. Effects of on-line vortex cooling on the microstructure and mechanical properties of wire arc additively manufactured Al-Mg alloy. *Metals* **2020**, *10*, 1004. [CrossRef]
35. Starink, M.J.; Li, X.M. A model for the electrical conductivity of peak-aged and overaged Al-Zn-Mg-Cu alloys. *Metall. Mater. Trans. A* **2003**, *34*, 899–911. [CrossRef]